Available online at www.garmian.edu.krd

Passer Journal

Passer 4 (Issue 2) (2022) 113-126

http://passer.garmian.edu.krd/

Biosynthesis and Characterization of ZnO Nanoparticles by using Leaf Extraction of Allium Calocephalum Wendelbow Plant

Amad Nori Abdulqudos[1], Ahmed Fattah Abdulrahman[1*]

[1]*Department of Physics, Faculty of Science, University of Zakho, Duhok, Kurdistan Region, Iraq*

Received 07 June 2022; revised 06 August 2022;
accepted 08 August 2022; available online 15 August 2022

doi:10.24271/psr.49

ABSTRACT

Zinc Oxide (ZnO) nanoparticles (NPs) were biosynthesized by using a leaf extract of Allium Calocephalum Wendelbow (ACW) plant. The impact of various zinc salts on the characteristic's properties of synthesized ZnO NPs and which salt is more suitable for the synthesis of the ZnO NPs were investigated. The used different zinc salts were Zinc Nitrate Hexahydrate (ZNH), Zinc Acetate (ZA), and Zinc Chloride (ZC). The properties of synthesized NPs were studied using a variety of characterization techniques. The FTIR analysis and UV-Visible spectroscopy of ACW plant leaf extract proved to suggest this extract is a better choice for the green synthesis of ZnO NPs. The UV–Visible spectra of leaf extract showed two distinct absorption peaks in the region of 262 nm and 350 nm at ambient temperature. The FE-SEM analysis revealed a spherical form of ZnO NPs having an (average) mean size in the range of (21.61-63.12) nm. Also, XRD results revealed the formation of a hexagonal wurtzite structure. The crystal size of produced ZnO NPs along the (002) diffraction peak was in the range of (16.91 to 28.19) nm for different Zinc salt. The EDX analysis shows that the produced ZnO NPs are very pure. The FTIR results displayed there is no obvious peak in the monitoring range, suggesting that the ZnO NPs created via using ACW Leaf Extract. Also, the UV-Vis. results of ZnO NPs showed that the sharpness peak in exciton absorption region, and UV absorption edge were found (381-397) nm, which is corresponding to the E_g of the ZnO NPs, and the investigated E_g of ZnO NPs was in the range of (3.12-3.25) eV. In addition, from all obtained results of the fabricated ZnO NPs, the ZnO NPs synthesized from zinc salt which is the Zinc Nitrate Hexahydrate showed the very high-quality and improved rather than the ZnO NPs synthesized from other zinc salts.

Keywords: Zinc Oxide, Nanoparticles, Allium Calocephalum Wendelbow Plant, Zinc Salts, Green Synthesis.

1. Introduction

Nanotechnology is a relatively young science. This can affect a lot of things. Due to their size and shape, nanomaterials offer a wide range of uses. They consume long piqued the curiosity of scientists in both the applied sciences and basic. Nanoscale semiconductors have gotten a lot of press in recent years because of their unique characteristics in employing optoelectronic applications. Adaptable semiconductors by significant optical transparency moreover luminescence in the UV–Visible (UV–Vis) areas include zinc oxide nanoparticles (ZnO)NPs, among other nanoparticles[1]. Because of their remarkable thermal durability and chemical, these nanoparticles have become more essential in current years[2]. The Zinc oxide is metal oxide n-type semiconductor[3]. Due to the own excellent properties such as direct energy band gap (3.37 eV), non-toxic, available, low cost and large area of applicability of ZnO NPs in different fields, the interest of ZnO NPs has increased in the last few years[3, 4]. Recently, there are huge studies that have been reported its use in the field of photocatalyst, novel sensors, antibacterial, biomedical engineering, development in the cancer therapies field, implant coating, wound healing, and tissue regeneration[4].

Several ways have been devised for producing ZnO NPs, such as precipitation methods, ultrasonic conditions, microwave-assisted techniques sol-gel, spray pyrolysis, chemical vapor deposition, and hydrothermal[5-8]. These kinds of preparations need a lot of energy and contain poisonous and harmful compounds, which might pose a biological risk. Biological approaches are more popular since they are typically less expensive, clean, one-step, very active, and safe[9].The biosynthesis approaches, in comparison to other physicochemical processes, generate nanoparticles with more defined sizes and forms[10]. Natural

* Corresponding author
E-mail address: ahmed.abdulrahman@uoz.edu.krd (Instructor).
Peer-reviewed under the responsibility of the University of Garmian.

chemicals in biological systems have significant and multifaceted involvement in NPs formation, acting by way of capping agents in the direction of keeping them stable. According to a literature review, plants offer major benefits in comparison to other biological systems. Because they are situated easily to use and widely accessible, plant extracts create more stable nanoparticles than synthesized nanoparticles[11].

Plant biological components are commonly used to manufacture Nanoparticles as plant extracts. Components of Plants, for example, seed, stem, root, and leaf, are commonly used in the production of metal-based NPs. Furthermore, the extract of plants contains phenolic acids, terpenoids, proteins, sugars, bioactive polyphenols, alkaloids, etc., They contribute significantly to the reduction of metallic ions also stabilizing them later[12]. Plant-mediated NPs biosynthesis may be divided obsessed into three stages(phases): reduction phase, growth phase then stabilization phase[13]. A reduction phase is the most critical step in recovering metal ions from salt precursors via plant metabolite interaction; biomolecules with the ability to reduce. The metal ions are converted from monovalent in the direction to divalent oxidation states, and subsequently, nucleation for reduced metal atoms takes place[14]. Formerly the growth phase as soon as isolated metal atoms recombine to produce metal nanoparticles though, metal ions undergo further biological reduction. While extensive nucleation may promote aggregation of generated nanoparticles, the growth phase improves the thermodynamic stability of nanoparticles morphologies that vary. The stabilization phase remains the last step in the biosynthesis of nanoparticles. When nanoparticles are coated with plant metabolites, they develop their most strongly beneficial and consistent form[12].

Several features of the solution combination, for example the reaction solution's PH, the concentration of plant extract, the concentration of metal salt, etc., Extra reaction conditions, for instance, reaction temperature and time, have a considerable impact arranged the quality, shape, also size of biosynthesized nanoparticles (NPs)[15]. Because zinc oxide (ZnO) remains one of the furthermost popular researched semiconductor metal oxides, it was investigated in this study. Through a high band-gap of 3.37 eV also an exciton binding energy of 60 meV, ZnO is a semiconductor material[16]. Wurtzite structure and Aside from its semiconductor properties, ZnO has intriguing piezoelectric properties[12], oxidizing[17], antibacterial, and also photo-catalytic characteristics[11]. Various plant extracts were employed trendy the green synthesis of ZnO NPs, including Euphorbia Milii, Tecoma castanifolia, Pisonia grandis R.Br., and so on[18-20]. Also, Arpita Dey et. al. synthesized the ZnO NPs by using a green method by employingleaf extract of Thryallis glauca (Cav.) Kuntze and they study their role as antibacterial and antioxidant applications. They found that the ZnO NPs were grown with wurtzite hexagonal structure less than 50 nm and the antioxidant analysis by DPPH assay illustrated an excellent free radical scavenging activity. The prepared ZnO NPs tested against pathogenic Escherichia coli, Pseudomonas aeruginosa, Staphylococcus aureus, and Bacillus subtilis did not show any antibacterial activity[21]. Abdullah M Abdo, et. al. prepared the green ZnO NPs by utilizing the Pseudomonas aeruginosa and they have investigated the activity of the ZnO NPs in against Pathogenic Microbes and Common House Mosquito, Culex pipiens[22]. The effect of the green method on the fabrication of ZnO NPs by using Aqueous Leaf Extracts of Coffee (Coffea arabica) was investigated by Saka Abel, et. al.[23]. They reported that the coffee leaf extraction serves as a reducing agent for the stability of the particle length, where its medicinal value outcome showed an important antibacterial of the pathogenic type which appeared on the wound. The present research deals with the green synthesis of ZnO NPs as well as its application in toxicity reduction[23]. Anatol Degefa et. al. obtained the effect of the different vegetable's extracts such as onion, cabbage, carrot, and tomato on the properties of ZnO NPs synthesized by using the green method for using Dye-Sensitive Solar Cells. They reported that the usage of the green produced ZnO NPs with creating dye sensitivity solar cell is a simple and viable way for the well-being of our future. Also, the ZnO nanoparticles can be used as intelligent weapons toward a wide range of drug-resistant microbes, as well as a capable antibiotic replacement[24]. Also, Alaa Falih, et. al. used the fresh and dry alhagi plant extract for fabrication of the ZnO nanoparticles by employing green method[25]. In addition, the green fabrication of zinc oxide NPs by using leaf extract of Cayratia pedata was reported by Ashwini Jayachandran et. al. They investigated that the nano Zinc oxide of varying sizes was obtained through wet chemical synthesis, and the average size was found to be 52.24 nm[26].

In this research, the ZnO NPs were biosynthesized by using leaf extract of Allium Calocephalum Wendelbow (ACW) plant, Also, the impact of the three different zinc salt as a precursor on ZnO NPs' characteristics synthesized via the green process was obtained and reported. The significant of the difference between zinc salt on ZnO NPs quality and which zinc salt is more appropriate of green synthesis of ZnO NPs have been investigated. The significance of this study is that the biosynthesis of ZnO nanoparticles and the Allium Calocephalum Wendelbow leaf plant which can be used for many uses such as; solar cell, photocatalyst activity, and eliminating pollutants in water, comatic, and medical (the antibacterial) applications.

2. Materials and Methods

Without any additional purification, every solvent and chemicals were acquired since Sigma-Aldrich. The used chemicals are Zinc Nitrate hexahydrate ($Zn(NO_3)_2.6H_2O$) which has a molecular weight of 297.48 g/mol, Zinc acetate dihydrate ($Zn(CH_3CO_2)_2{\cdot}2H_2O$) through a molecular weight of 219.51 g/mol, Zinc chloride ($ZnCl_2$) utilizing a molecular weight of 136.30 g/mol, and Sodium hydroxide (NaOH) molecular weight of 40.00 g/mol. The Ultrasonic (S15H, Germany); Heater-Stirrer (MR Hei- End, Germany); Oven (Memmert 100-800, Germany); Rotary evaporator (4003 Heidolph, Germany); Centrifuge (EBA 20 Hettich, Germany) were used for all preparation and synthesis ZnO nanoparticles.

2.1 Preparation of the Allium Calocephalum Wendelbow Plant Extract

Allium Calocephalum Wendelbow (ACW) family (Amaryllidaceae) commonly known. This species is accepted, in addition, its native range is South-Earth Turkey to North Iraq also, obtained in the spring season in Amedi korajar Mountain

(Latitude 36°11'28.9"N and Longitude 43°58'42.3"E) exactly at Duhok, Iraqi-Kurdistan Region (April 2021). The leaves were allowed to dry after being cleaned. In a mortar, the dried leaves were crushed, and 50 g of leaves powdered were combined through 500 mL distilled water besides boiled for 15 minutes at 75°C employing a heater and stirrer. Before being stored for future use, to eliminate plant debris and contaminants, the liquid was centrifuged and filtered.

2.2 Biosynthesis of Zinc Oxide Nanoparticles

The ZnO NPs were prepared by using the biosynthesis process and extracted from Allium Calocephalum Wendelbow for varying zinc salts (Nitrate, Acetate, also Chloride). After preparing a plant extract as mentioned above, the 50 ml of the prepared extract was utilized and added drop by drop to the 0.1 mol zinc nitrate hexahydrate [Zn (NO3)2·6H2O] solution for 30 min at 60 C°. The pH of the above mixture has been controlled and adjusted by adding the Sodium Hydroxide (NaOH) to a pH of 8 until the mixture's color becomes milky, which means the nucleation process and the reaction started of ZnO nanoparticles. Afterward, the mixture was continuously stirred aimed at 1 hour at 60 degrees Celsius, until it transformed obsessed by a brownish paste. The temperature of the reaction required a significant impact on the yield of NPs, with 60C°for 3 hours yielding the best results and the corresponding sample was labeled as **(a)**. Then ZnO NPs powder was gained for zinc Nitrate[27, 28]. Therefore, the generation of ZnO NPs of specified shape and size was noticed by the white color for the solution grows. The sedimentation of the growth solution remains separated via using centrifugation at 10000 rpm besides the ZnO NPs Methanol was used to clear the solid powder, and ethanol Use distilled water many times to eliminate any contaminants otherwise organic materials. However, the same procedure and steps mentioned above for Zinc Nitrate have been used and applied for the biosynthesis of ZnO nanoparticles employing the Zinc salts such by way of Zinc acetate dihydrate (Zn $(CH_3CO_2)_2 \cdot 2H_2O$) also Zinc chloride ($ZnCl_2$) and were labeled as **(b)** and **(c),** respectively. Finally, for their samples the paste for them was blazed intended for approximately 2 hours at the side of 500°C in a furnace, in addition, to distilled water, the residue was cleaned many times with ethanol[13, 27]. The ZnO The powder was then dried at 100°C. as shown in Figure 1. Then ZnO NPs were obtained and they were ready for characterization.

2.3 Characterization of Zinc Oxide Nanoparticles

The UV-Visible double-beam spectrophotometer was utilized to investigate the optical properties of ZnO. Agilent Technologies' Carrier Series UV-Visible double-beam spectrophotometer (Cary 100 UV-Vis) has wave lengths ranging from 200 to800 nanometers and were used to research and obtain features of the optical character of the leaf plant extract and ZnO NPs. The unique functional groups existing in the Allium Calocephalum Wendelbow leaf plant extract also synthesized Zinc oxide nanoparticles for different Zinc salts were obtained and examined via using the Fourier Transform Infrared Spectroscopy (FTIR) Nicolet IS 10 (Thermo Scientific, the USA in the range of (400-4000) cm^{-1}. The Field Emission Scanning electron microscopy (FE-SEM) (Carl Zeiss AG (Supra 55VP) through a voltage acceleration of 5-30 kV) in addition Energy-dispersive X-ray Spectroscopy (EDX) were accustomed to examine besides investigating respectively the product's morphology surface, size, orientation shape and chemical composition of ZnO nanoparticles. The crystal structure and size, the epitaxial growth goodness (quality), the stress, and the strain, of fabricated ZnO NPs from different zinc salts have been studied and examined by utilizing the system of high-resolution X-Ray diffraction (HR-XRD) by model Pro MRD, PAN X-Pert. The wavelength (λ) of CuK radiation (1.54050 Angstrom) with (2θ) of the scanning range (20^o – 80^o).

3. Results and Discussion

3.1 Characterization of Allium Calocephalum Wendelbow Leaf Extract

Recently, acceptable to maintain control of the shape, morphology, orientation also size of ZnO nanoparticles, the researchers were utilizing the phytochemicals present in one plant for fabricating nanoparticles by using the green method[12]. The phytochemicals that were present in each part of Metal ions are reduced in the direction of metal nanoparticles by an extract of the plant. As a result, at the same time, the plant extract is affected by way of a reducing also stabilizing agent[27]. To study and obtain this process of reaction, the UV-Visible. spectroscopy has been used. The Spectrum of UV–Vis. spectroscopy showed a peak absorption surface plasmon resonance (SPR) also captures electron oscillations in the conduction-band reacting Metal ion reduction and nanoparticle production is represented by electromagnetic waves[12].

Figure 2 displays the UV-Visible spectra plant extract of leaf of the Allium Calocephalum Wendelbow. One can notice there are two maximum peaks were obtained at 262 nm also 350 nm, which might be linked to the dominant phytochemicals that present in the Allium calocephalum Wendelbow leaf plant which possible Because OH groups are abundant, stabilizing agents, bio-reducing can be used to make nanoparticles[29]. Because they are antioxidants and free of toxic substances, these phytochemicals stay exceptionally capable of lowering metal ions also their stabilization at the dimension of the nanoscale. They're also capable of creating nanoparticles in a variety of sizes in addition forms[30]. The zinc ions create a Zn (OH)2 combination through the OH groups. Three pathways are involved in the phase change from Zn (OH)2 to ZnO., i.e., reprecipitation of dissolution, trendy situ crystallization, in addition, solid-solid phase transition It has furthermore been hypothesized that water is lost from the lattice throughout the solid-solid for phase transition by Wang et al.[31].

The functional groups associated with these reductive biomolecules were investigated employing Fourier transform infrared (FTIR) ZnO NPs and plant extract spectrum, along with, identifying the functional groups that help reduce ZnO obsessed by nanoparticles[12, 27]. The spectrum of FTIR for the Allium Calocephalum wendelbow leaf extract is shown in Figure 3 and contains several peaks visible throughout the entire range. Generally, there are two regions in the spectrum of FTIR. i.e., the (0-1500) cm^{-1} is the region of fingerprint also the range of (1800-4000) cm^{-1}remains the functional group region.

Infrared research was used to assess the quality and provenance of the nanoparticles, as well as the presence of phytochemicals trendy the extract. The FT-IR spectra provide information on the nature of inside samples bonding trendy altogether stages of matter[32-34]. Primarily, the peak absorption at around 3549 cm^{-1} is qualified to Dimeric OH (vibration of stretching). The peak around 3429 cm^{-1} is accredited near the H-bonded OH stretch or Hydroxy group beside near 3387 cm^{-1} is peak qualified Aliphatic Primary amine via NH stretch vibration alongside 3367 cm^{-1} is peak competent Aromatic Primary amine via NH stretch. also, the narrow Around absorption peak of 2926 cm^{-1}stays credited in the direction of Methylene C-H asym vibration too the peak of 1747 cm^{-1} is the carbonyl compound of (Ester). furthermore, the peak around 1647 cm^{-1} is a secondary amine >N-H bend. Another peak found in the scheme is a 1417 cm^{-1} vinyl C-H trendy-plane bend. However, the peak of 1051 cm^{-1} is Alkyl-substituted ether or O-H stretches vibration while the peak around 954 cm^{-1} is Aromatic C-H trendy-plane bend. Also, the peak of approximately 690 cm^{-1} is Thiols and thio-substituted compounds or CH2-S- (C-S stretch). Another two pecks instituted in the scheme of (ACW) 576 cm^{-1} and 445 cm^{-1} are Disulfides (C-S stretch) also Aryl Disulfides (S-S stretch). These chemicals may be responsible and aimed at the production of nanoparticles via reducing metal or else metal oxide ions[35].

3.2 Characterization of ZnO Nanoparticles (NPs)

In this research, different characterization performances have been used in the direction of study and designate the shape, size, morphology, distribution, crystal structure, particle size, chemical composition, ZnO nanoparticles optical characteristics, and energy band gap by using the leaf plant extraction method.

3.2.1 Field Emission Scanning Electron Microscopy (FESEM)

The FESEM analysis has been used to analyze the surface morphology (top-view), size, shape, orientation, and distribution of biosynthesized ZnO nanoparticles from different zinc salts as shown in Figure 4. From Figure 4, the synthesized ZnO nanoparticles exhibited grown up in a nano-sized range, a homogenous distribution and a shape spherical of ZnO NPs fabricated from the zinc nitrate hexahydrate. The numerous Salts utilized altered the morphology and size of nanoparticles, as stated via the FESEM data. The ZnO molecules grow slowly when zinc nitrate is employed as a salt, generating near-spherical-clusters forms that pile up like bullets. Instead, when zinc acetate is utilized in place of salts, massive nanoparticles with the agglomeration of ZnO nanoparticles, in addition to many quasi-spherical shaped ZnO nanoparticles, can be seen in the image. The electrostatic attraction and polarity of ZnO NPs cause this agglomeration. moreover, the shape of the surface for Chloride ZnO NPs in the creation of spongy structure is vividly seen in the greatly enlarged FESEM scheme of biosynthetic nanoparticles. By considering the NPs as forms besides estimating the distribution of particle size as of the deduced area by using Image J software using frequency histogram of ZnO nanoparticles distributions as shown in Figure 4 (d, e besides f). The average size particle for the ZnO NPs as-synthesized Using a Gaussian distribution in the direction of matching the related histogram data. From the frequency histogram of ZnO n distributions, the average particle size of biosynthesized ZnO NPs remained 29.61 nm, 36.75 nm, and 63.12 nm aimed at Zinc Nitrate, Zinc Acetate, also Zinc Chloride, correspondingly. From the obtained FESEM results, one can conclude that the ZnO NPs synthesized from zinc nitrate hexahydrate shows the high-quality such as same size, uniform spherical shape, and uniform distribution density compared to the ZnO NPs synthesized from other two zinc salts.

Green synthesis nanoparticles (NPs), including ZnO NPs, are frequently agglomerated. This is a result of biosynthetic NPs' larger surface area, which causes agglomeration or aggregation because of their long-term affinity[36]. It has been shown that ecological considerations have a considerable influence on NP aggregation and stability. As a result, during the nanoparticle production process, NPs adhere to one another and spontaneously form asymmetrical clusters[3]. The concentration of plant extract or else biomass, the salt concentration, the reaction or growth time, the pH, also the temperature of the solution are all critical factors in the production of ZnO NPs. In place of a result, calibrating these growth factors is essential for achieving the best NPs shape and size aimed at maximal manipulation and request[12, 27].

3.2.2 Energy-Dispersive X-Ray Spectroscopy (EDX)

The EDX spectroscopy analysis has been used to study the elemental chemical compositions of the biosynthesized ZnO nanoparticles by using Leaf extract of Allium Calocephalum Wendelbow Plant for different Zinc salt as shown in the Figure 4. From Figure 5, the technique of EDX displays the attendance of O and Zn, which, excluding the presence of any flaws or else substrate signs in line with EDX limits, corresponds to the direction of the attribute composition of ZnO[27]. The spectra of EDX exhibited two peaks robustly aimed at Zinc (Zn) about 1.1 keV also 8.7 keV, similarly, and a singular peak for oxygen using ~ 0.5 keV, ZnO NPs have unique properties[12]. For all produced ZnO NPs samples from various reactants, the atomic ratio between oxygen and zinc was nearly the same (zinc salts). The molecular ratio (MR) of Zinc: Oxygen in the formed NPs was roughly 1:1, as established via quantitative characterizations of (EDX), showing that the generated NPs were pure ZnO. EDX analysis was used in the direction to determine the atomic percentage for ZnO NPs composition are Zn (83.54%) and O (16.56%) for Zinc Nitrate, Zn (84.36%) and O (15.66%) for Zinc Acetate, and Zn (84.65%) and O (15.35%) Zinc Chloride.

3.2.3 X-Ray Diffraction (XRD) Analysis

The technique of X-ray diffraction was utilized to validate the presence of Nanoparticles also to examine their structural features[37]. The ZnO wurtzite hexagonal phase was detected by way of the diffraction peak is completely XRD patterns. Furthermore, Other contaminants did not show any diffraction peaks., showing that the ZnO nanoparticles were grown as the ZnO nanocrystal phases with high purity. From Figure 6 and Tables 1, 2, and 3 the biosynthesized ZnO NPs linked with Allium Calocephalum Wendelbow exhibited strong peaks with 2θ values determined at (31.9910°, 34.6996°, and 36.5253°) Zinc Nitrate, (31.9219°, 34.6152°, and 36.4374°) Zinc Acetate, and (31.8865°,34.629°, and 36.4562) Zinc Chloride which is indexed as (100), (002), and (101) planes. These peaks corresponded to those on the data card. (JCPDS-98-002-9272). ZnO NPs have a

perfect crystalline structure situated shown by the thin and strong peaks of diffraction. From Figure 6 (a and b), one can conclude that the diffractions peaks along (101) plane are more dominant and stronger peaks, and the obtained XRD results behaviors are good agreement with previous studies[12, 21-26]. While Figure 6 (c) shows a higher and stronger diffraction peak at the plane of (100), which indicated that the most of ZnO NPs were grown at the plane (100) and the obtained results behavior are in good agreement with previous studies[38].

The full width at half maximum (FWHM) value for XRD spectra may be used to analyze the crystal quality and compositional phase distribution of the produced ZnO NPs structure. The Scherrer equation is used to compute the average crystallite size from the XRD data[39]:

$$D = \frac{k\lambda}{\beta\cos\theta} \quad (1)$$

where β, θ, λ, K, and D, are full width at half maximum (FWHM) of the peak, diffraction angle, the wavelength of the X-ray beam, the factor of crystallite size shape which is 0.9, and D is average crystalline size, correspondingly.

The obtained average crystallite size along the strong diffraction peaks (100), (002), and (101) for Zinc Nitrate were determined to be 21.15 nm, 20.9966 nm, and 21.2242 nm, respectively, for Zinc Acetate 16.91 nm, 20.9929 nm, and 21.2488 nm, and for Zinc Chloride 28.19 nm, 20.9911 nm, and 48.5969 nm. The X-ray diffraction study established the presence of uniform smaller nanoparticles than the examination of SEM had exposed. The aggregation of smaller sample nanoparticles created the bigger ZnO nanoparticles, which were noticed using X-ray diffraction. The X-ray diffraction technique remained used to identify nanoparticles with lower diameters[12]. The structural properties, intensity, lattice constants (a & c), peak position (θ), also the internal strains (ξ_c, ξ_a) for ZnO NPs lengthways strong diffractions peaks (100), (002), and (101) for different Zinc Salts are registered in Table1. The lattice constants (*a*&*c*) of the ZnO hexagonal structure are found employing Bragg's law[40]:

$$a = \sqrt{\frac{1}{3}}\frac{\lambda}{\sin\theta} \quad (2)$$

$$c = \frac{\lambda}{\sin\theta} \quad (3)$$

Wherever λ is the wavelength for the X-ray source addition θ is the angle for a diffraction peak.

The strains (ξ_c) and (ξ_a) of the ZnO along the a-axis and c-axis, respectively are considered since the following equations[41]:

$$\varepsilon_a = \frac{a-a_o}{a_o} \times 100\% \quad (4)$$

$$\varepsilon_c = \frac{c-c_o}{c_o} \times 100\% \quad (5)$$

Wherever a_o besides c_o are denoted the standard lattice constants aimed at the database, there exist unstrained ZnO NPs. The variances of strains (ξ_c) besides (ξ_a) by way of exhibiting in Table1 are owing to the variance in inter-planar spacing vales by way of a resulting mismatch between substrate and crystal growth. A Compressive strain is represented by a negative strain value, implying lattice contraction., whereas a positive strain value corresponds to tensile strain and shows lattice constant expansion[39]. The inter-planer distance of ZnO nanoparticles length ways and stronger diffraction peaks has been discovered following Bragg's law[40], and a summary of its findings is trendy in Table 1.

$$\frac{1}{d^2} = \frac{4}{3}\left(\frac{h^2+hk+k^2}{a^2}\right) + \frac{l^2}{c^2} \quad (6)$$

Wherever h, k, and l be situated Miller indices as of X-Ray diffraction peaks.

The dislocation density (δ) This indicates the number of defects caused by internal strain and substrate-crystal growth mismatch, and is computed using the following equation[37]:

$$\delta = \frac{1}{D^2} \quad (7)$$

Wherever D is crystallite size

Similarly, the effect of a different zinc salt on hexagonal cell volume also ZnO nanoparticles bond length is listed trendy Table 2 and is determined using the formulae below[39]:

$$L = \sqrt{\frac{a^2}{3} + \left(\frac{1}{2} - u\right)^2 c^2} \quad (8)$$

Wherever u is a parameter associated with the c/a ratio, u is a unit of measurement measuring how far one atom has moved in the direction of the next, lengthways the 'c' axis also it is assumed via using the formula below[41]:

$$u = \frac{a^2}{3c^2} + 0.25 \quad (9)$$

As well, a hexagonal cell's volume (V) also the following formula was used to compute[40]:

$$V = \frac{\sqrt{3}}{2}a^2c \quad (10)$$

The existence dissimilarity of both bond length and volume is owing to the diversity in the position of the peak 2θ along dissimilar stronger peak diffraction for the reason that both are directly dependent on the lattice parameters a and c, as well as the value of 2θ[39].

3.2.4 Fourier Transform Infrared (FTIR) Spectroscopy Analysis

The spectrum of FTIR is employed in the direction of examining the purity, besides composition for ZnO NPs produced via biosynthesis as shown in Figure 7. The mentioned figure shows that there was no discernible peak in the monitoring range that indicated the purity of the ZnO nanoparticles generated via using Allium Calocephalum Wendelbow Leaf Extract. The broadband at 620 cm^{-1}disappearedZnO nanoparticles synthesized. An additional peak was designed at 421 cm^{-1}ZnO nanoparticles are formed as a result of this process, bonding vibrations of zinc and oxygen[42, 43].

For three biosynthesized ZnO NPs samples, there is a succession of peak absorption ranging from 1000 to 4000 cm^{-1}. To remain additional exact the peaks observed at 2964 are owing to the Methyl C-H asym. / Sym stretch. The band's presence of three by

2023 cm^{-1} is in agreement through the presence of three crystallographically different OH groups, and the 2023 cm^{-1} is an aromatic combination band beside Isothiocyanate (-NCS). Also, two absorption bands were detected in 1975 and 1721. While the band by 1975 cm^{-1}looks like the Aromatic combination bands, However, another three peaks were detected at (1431,1140, and 1025 cm^{-1}). At the peak 1431 cm^{-1} is a common inorganic ion for Carbonate ion beside at peak 1140 cm^{-1} is a secondary amine or a CN stretch alongside at peak 1025 cm^{-1} is Aliphatic Fluoro compounds or C-F stretch. Finally, there are four peaks were distinguished (879, 700, 620, and 421 cm^{-1}). At peaks, 879 and 700 cm^{-1} were peroxides or C-O-O- stretch and Methyne (>CH-) for skeletal C-C vibrations. furthermore, peaks 620 and 421 cm^{-1} were noticed as Alkyne C-H bend also Aryl disulfides (S-S stretch). In addition, the peak 1069 cm^{-1}isthe same range in group Aliphatic fluoro compounds or C-F stretch was observed for ZnO NPs synthesized as of Zinc Acetate also Zinc Chloride.

3.2.5 Optical Properties of ZnO Nanoparticles

The optical properties of ZnO nanoparticles produced in the green from different Zinc salts were studied based on the use of UV-Visible spectrometers to observe optical absorptions via ZnO NPs samples. The optical absorption spectra of ZnO NPs that have been fitted using Allium Calocephalum Wendelbow leaf extract for different zinc salts with a range of wavelength between 300 nm towards 800 nm by way of exposure in Figure 8. ZnO has strong UV absorption and high absorbance at wavelengths below 400 nm, as well as remarkable clarity and a small visible absorption range[44]. Impurities in ZnO NP, for instance, interstitial Zn atoms and oxygen vacancies that pe as donor defects, are responsible for the low absorption values by long wavelengths[45].

Exciton absorption and a strong UV absorption edge were detected trendy the range (of 381-397) nm, which stays conforming to the optical energy band-gap (Eg) of the ZnO nanoparticles. Because of the surface plasmon resonance (SPR), The fabrication of monodispersed ZnO NPs was established when the peak sharpened[12]. Instead of following the rule of thumb, the highest peak absorption of ZnO NPs was found to be located between 350to400 nm. The assessed value was lower than that of bulk ZnO assumed employing 381-397 nm[46] and also showed a blue change in excitonic absorption, indicating a small quantum confinement effect[12].

The optical bandgap energy of ZnO nanoparticles fabricated at different Zinc salts was derived by extrapolating the linear component of (αhν)2 against h using transmittance spectrums and the Tauc formula[12, 27], as shown in Figure 9.

$$(\alpha h\nu)^2 = A(h\nu - E_g)^n \quad (11)$$

Wherever α is the absorption coefficient, hν is the energy photon, A is constant, E_g is the optical band gap energy also n depends on the transmission kind (equals 1/2 for allowed direct transmission). Aimed at the transmittance spectrum the (α) coefficient container stays considered via[41].

$$\alpha = \frac{\ln(\frac{1}{T})}{d} \quad (12)$$

Wherever T is the transmittance for ZnO samples, also d is the thickness of the sample

The transition region is roughly 3.2 eV, according to the diagrams, and corresponds to the straight transition band between the valance and conduction bands, which represents the optical energy gap of the ZnO semiconductor[44]. Regarding the plot, precisely examined the band-gap energy of ZnO nanoparticles is approximately 3.25 eV, 3.18 eV, and also 3.12 eV aimed at Zinc Nitrate Hexahydrate, Zinc Acetate, and Zinc Chloride, correspondingly. Since some components of Cover/modify the surface with plant extract moreover reduce the band-gap for the nanoparticles, a drop trendy the band-gap stays predicted as a result of utilizing the plant extract[47]. This finding, principally in green nanoparticles, is not incompatible with quantum confinement events. Biosynthesized nanoparticles are often more reactive than nanoparticles made by conventional techniques[48]. The overall greater direction of a rise in electron inhabitants in lower energy bands can be linked to the direction of particle reactivity in the quantum domain way of a result of the smaller separation of states of energy[49]. Metal NPs have diameters that are substantially smaller than visible light wavelengths. They interact with light, in addition can absorb or else disperse it. Metal oxides inside bulk have a broad band-gap and also have a limited capacity to interact[27]. However, when their dimensions are reduced, they develop more sensitivity, their interrelationship ability may also be determined by their reflection and absorption capacities. The absorption peak intended for ~40 nm ZnO NPs have been labeled by Singh et al. [50] at 361 nm (3.44 eV) and 3.44 eV to make ZnO NPs chemically[51], correspondingly.

8. Conclusion

In a nutshell, the high-quality ZnO NPs were successfully biosynthesized by using the green method using the aqueous extract leaves of the Allium Calocephalum Wendelbow (ACW) plant. The impact of several zinc salts as a precursor with plant extract on the properties of synthesized ZnO nanoparticle have been investigated. The UV-visible spectrum revealed a characteristic peak at 350 nm that is unique to ZnO NPs. The synthesis procedure' efficiency was validated by the XRD data demonstrating the fabrication of hexagonal wurtzite-structured single-crystalline ZnO NPs. The average size for ZnO NPs fabricated via zinc nitrate, zinc acetate, and zinc chloride was (21.61, 36.75, and 63.12) nm, respectively. Also, the XRD and FE-SEM results corroborated and demonstrates that ZnO NPs synthesized with zinc nitrate were grown near-spherical with agglomeration, spherical, and spongy similar structures. The presence of oxygen and zinc in the produced ZnO NPs was verified by EDX data. The creation of ZnO was demonstrated by FT-IR experiments, which also revealed that the plant extract contained a variety of phytochemicals which serve by way of a stabilizing and capping agent aimed at ZnO NPs produced. It is obvious from the data that the precursors (salts) had an important influence on the surface structure, size, orientation, quality crystal structure and shape of ZnO NPs. Our findings support the use of Allium Calocephalum Wendelbow for the production of ZnO NPs in a quick, simple, and environmentally friendly manner. In addition, from all investigated results of the biosynthesized ZnO NPs, the ZnO NPs biosynthesized from zinc salt which is the zinc

Nitrate hexahydrate showed the very high-quality and improved rather than the ZnO NPs synthesized from other zinc salts.

Conflict of interests

The authors declare no conflict of interest for this study.

Acknowledgments

Amad Nori Abdulqodus would like to thank the University of Zakho-Zakho Duhok, Iraq, for being an MSc. student and fully supported by them. The authors would like to thank the Department of Biophysics, Institute for Research and Medical Consultation (IRMC), Imam Abdulrahman Bin Faisal University, Dammam, Saudi Arabia, Center of Nanotechnology and Material Science, Department of Physics, University of Zakho- Zakho, Iraq, and Soran research center for providing all the facilities to perform the research work. In addition, the authors are gratefully to Dr. Azeez A. Barzanjy at the Department of Physics Salahaddin University-Erbil, Dr. Samir M. Hamad at Soran University-Iraq and Mr. Shinwar A. Idrees at Chemistry Department, University of Zakho-Iraq for their valuable assistant throughout this investigation.

References

[1] S. Fakhari, M. Jamzad, and H. K. Fard. “Green synthesis of zinc oxide nanoparticles : a comparison,” Green Chemistry Letters and Reviews, vol. 12, no. 1, 2019. https://doi: 10.1080/17518253.2018.1547925.

[2] P. Nunes, B. Fernandes, E. Fortunato, P. Vilarinho, and R. Martins. “Performances presented by zinc oxide thin films deposited by spray pyrolysis,” Thin Solid Films, vol. 337, pp. 176–179, 1999.

[3] H. Agarwal, S.V. Kumar, S. R. kumar. “A review on green synthesis of zinc oxide nanoparticles An eco-friendly approach”, Resource-EfficientTechnologies, vol 3, pp. 406–413, 2017.

[4] M. Bandeira, M. Giovanela, M. Roesch-Ely, D. M. Devine, and J. Da-S. Crespo. “Green synthesis of zinc oxide nanoparticles: A review of the synthesis methodology and mechanism of formation”, Sustainable Chemistry and Pharmacy,vol.15, pp. 100223, 2020.

[5] A. K. Zak, M. E. Abrishami, W. H. A. Majid, R. Yousefi, and S. M. Hosseini. “Effects of annealing temperature on some structural and optical properties of ZnO nanoparticles prepared by a modified sol-gel combustion method”, Ceramics International, vol. 37, no. 1, pp. 393–398, 2011. https://doi: 10.1016/j.ceramint.2010.08.017.

[6] C. Lu and C. Yeh. “Influence of hydrothermal conditions on the morphology and particle size of zinc oxide powder”, Ceramics International, vol. 26, pp. 351–357, 2000.

[7] K. Okuyama and I. W. Lenggoro. “Preparation of nanoparticles via spray route,” Chemical Engineering Science, vol. 58, pp. 537–547, 2003. https://doi: 10.1016/S0009-2509(02)00578-X.

[8] Y. Wang, C. Zhang, S. Bi, and G. Luo. “Preparation of ZnO nanoparticles using the direct precipitation method in a membrane dispersion microstructured reactor,” Powder Technology, vol. 202, no.1-3, pp. 130–136, 2010. https://doi: 10.1016/j.powtec.2010.04.027.

[9] S. Saif, A.Tahir, T. Asim, Y. Chen, M. Khand, S. F. Adild. “Green synthesis of ZnO hierarchical microstructures by Cordia myxa and their antibacterial activity”, Saudi J Biol Sci, vol. 26, pp. 1364–1371, 2019.

[10] P. Raveendran, J. Fu, S. L. Wallen, C. Hill, and N. Carolina. “Completely Green Synthesis and Stabilization of Metal Nanoparticles,” J. Am. Chem. Soc., vol.125, no. 46, pp.13940–13941, 2003

[11] S. Iravani. “Green synthesis of metal nanoparticles using plants,” Green Chemistry, vol. 13, pp. 2638–2650, 2011. https://doi: 10.1039/c1gc15386b.

[12] A.A. Barzinjy, H. H. Azeez. “Green synthesis and characterization of zinc oxide nanoparticles using Eucalyptus globulus Labill. leaf extract and zinc nitrate hexahydrate salt”, SN Applied Sciences, vol. 2, no.99, 2020. https://doi.org/10.1007/s42452-020-2813-1.

[13] J. Kim, Y. Rheem, B. Yoo, Y. Chong, K. N. Bozhilov, D. Kim, M. J. Sadowsky, H-G Hur., N. V. Myung. “Peptide-mediated shape-and size-tunable synthesis of gold nanostructures”, Acta Biomater, vol. 6, pp.2681, 2010.

[14] P. Malik, R. Shankar, V. Malik, N. Sharma, T. K. Mukherjee. “Green chemistry based benign routes for nanoparticle synthesis”, J. of Nanoparticles, vol. 2014, Article ID 302429, 14 pages, 2014. https://doi.org/10.1155/2014/302429.

[15] A. D. Dwivedi, and K. Gopal, “Biosynthesis of silver and gold nanoparticles using Chenopodiumalbum leaf extract”, Colloid Surface A, vol.369, pp.27–33, 2010.

[16] A. F. Abdulrahman, S. M. Ahmed, N. M. Ahmed, and M. A. Almessiere. “Enhancement of ZnO Nanorods Properties Using Modified Chemical Bath Deposition Method: Effect of Precursor Concentration”, Crystals, vol. 10, pp. 386, 2020. https://doi:10.3390/cryst10050386.

[17] A. F. Abdulrahman, S. M. Ahmed, S. M. Hamad, M. A. Almessiere, N. M. Ahmed, S. M. Sajadi. “Effect of different pH values on growth solutions for the ZnO nanostructures”, Chinese Journal of Physics, Vol. 71, pp.175-189, 2021. https://doi.org/10.1016/j.cjph.2021.02.013.

[18] S. Joghee, P. Ganeshan, A. Vincent, and S. I. Hong. “Eco-friendly Biosynthesis of Zinc Oxide and Magnesium Oxide Particles from Medicinal Plant Pisonia Grandis R . Br Leaf Extract and Their Antimicrobial Activity,”BioNanoScience, vol. 9, no. 2, 2018. https://doi.org/10.1007/s12668-018-0573-9.

[19] G. Sharmila, M. Thirumarimurugan, and C. Muthukumaran. “Green synthesis of ZnO nanoparticles using Tecoma castanifolia leaf extract: Characterization and evaluation of its antioxidant, bactericidal andanticancer activities,” Microchemical Journal, vol. 145, pp. 578–587, 2019. https://doi:10.1016/j.microc.2018.11.022.

[20] M. S. Yedurkar, D. K. Punjabi, B. C. Maurya, and A. P. Mahanwar. “ScienceDirect Biosynthesis of Zinc Oxide Nanoparticles using Euphorbia Milii Leaf Extract- A Green Approach,” Materials Today: Proceedings, vol. 5, no.10, pp. 22561–22569, 2018. https://doi: 10.1016/j.matpr.2018.06.629.

[21] A. Dey and S. Somaiah, “Green synthesis and characterization of zinc oxide nanoparticles using leaf extract of Thryallis glauca (Cav.) Kuntze and their role as antioxidant and antibacterial”, Microscopy Research and Technique, April 2022, https://doi.org/10.1002/jemt.24132.

[22] A. M. Abdo, A. Fouda, A. M. Eid, N. M. Fahmy, A. M. Elsayed, A. M. Khalil, O. M. Alzahrani, A. F. Ahmed, A.M. Soliman. “Green Synthesis of Zinc Oxide Nanoparticles (ZnO-NPs) by Pseudomonas aeruginosa and Their Activity against Pathogenic Microbes and Common House Mosquito, Culex pipiens”, Materials (Basel), vol. 14, no. 22, pp. 6983, 2021. https://doi: 10.3390/ma14226983.

[23] S. Abel, J. L. Tesfaye, R. Shanmugam, L. P. Dwarampudi, G. Lamessa, N. Nagaprasad, M.Benti, R. Krishnaraj. "Green Synthesis and Characterizations of Zinc Oxide (ZnO) Nanoparticles Using Aqueous Leaf Extracts of Coffee (Coffea arabica) and Its Application in Environmental Toxicity Reduction", J. of Nanomaterials, vol. 2021, ID 3413350, 6 pages, 2021. https://doi.org/10.1155/2021/3413350.

[24] A. Degefa, B. Bekele, L.T. Jule, B. Fikadu, S. Ramaswamy, L. P. Dwarampudi, N. Nagaprasad, K. Ramaswamy. "Green Synthesis, Characterization of Zinc Oxide Nanoparticles, and Examination of Properties for Dye-Sensitive Solar Cells Using Various Vegetable Extracts", Journal of Nanomaterials, vol. 2021, Article ID 3941923, 9 pages, 2021. https://doi.org/10.1155/2021/3941923.

[25] A. Falih, N. M. Ahmed, and M. Rashid. "Green synthesis of zinc oxide nanoparticles by fresh and dry alhagi plant", Materials Today Proceedings, vol. 49, no. 8, pp.3624-3629, 2022.

[26] A. J. Aswathy, T. R. Achuthsankar. S. Nair. "Green synthesis and characterization of zinc oxide nanoparticles using Cayratia pedata leaf extract", Biochemistry and Biophysics Reports,v ol. 26, pp. 100995, 2021.

[27] A. A. Barzinjy, S. M. Hamad, A. F. Abdulrahman, S. J. Biro and A. A. Ghafor. "Biosynthesis, characterization and mechanism of formation of ZnO nanoparticles using Petroselinum crispum leaf extract", Current Organic Synthesis,vol. 17, no. 1, 2020. https://doi.org/10.2174/1570179417666200628140547.

[28] M. Sathishkumar, K. Sneha, and Y. S. Yun. "Immobilization of silver nanoparticles synthesized using Curcuma longa tuber powder and extract on cotton cloth for bactericidal activity," Bioresource Technology, vol. 101, no. 20, pp. 7958–7965, 2010. https://doi: 10.1016/j.biortech.2010.05.051.

[29] P. Singh, Y. J. Kim, D. Zhang, D. C. Yang. "Biological synthesis of nanoparticles from plants and microorganisms", Trends Biotechnol, vol. 34, pp. 588–599. 2016.

[30] R. Hocine, J. Mazauric, K. Madani, L. Boulekbache-Makhlouf. "Phytochemical analysis and antioxidant activity of Eucalyptus globulus: a comparative study between fruits and leaves extracts", J. Chem. Eng Bio Chemistry, vol. 1, pp.23–29, 2016.

[31] Ovais, Ahmad I., Islam NU., Saravanan M, Ubaid MF, Ali M, Shinwari ZK, Green synthesis of silver nanoparticles via plant extracts: beginning a new era in cancer theranostics. Nanomedicine, vol. 12, pp.3157–3177, 2016.

[32] R. Norouzi, M. Hejazy, and A. Ataei. "Scolicidal effect of zinc oxide nanoparticles against hydatid cyst protoscolices in vitro," Nanomedicine Research Journal, vol. 4, no.1, pp. 23–28, 2019. https://doi: 10.22034/NMRJ.2019.01.004.

[33] V. Srivastava, D. Gusain, and Y. C. Sharma. "Synthesis, characterization and application of zinc oxide nanoparticles (n-ZnO)," Ceramics International, vol. 39, no. 8, pp. 9803–9808, 2013. https://doi: 10.1016/j.ceramint.2013.04.110.

[34] S. Zandi, P. Kameli, H. Salamati, H. Ahmadvand, and M. Hakimi. "Microstructure and optical properties of ZnO nanoparticles prepared by a simple method," Physica B: Condensed Matter, vol. 406, no.17, pp. 3215–3218, 2011. https://doi: 10.1016/j.physb.2011.05.026.

[35] J. P. Kim, I. K. Lee, B. S. Yun, S. H. Chung, G. S. Shim, H. Koshino, I. D. Yoo. "Ellagic acid rhamnosides from the stem bark of Eucalyptus globulus", Phytochemistry, vol. 57, pp.587–591, 2001.

[36] M. Sundrarajan, S. Ambika, K. Bharathi. "Plant-extract mediated synthesis of ZnO nanoparticles using Pongamia pinnata and their activity against pathogenic bacteria", Adv Powder Technol, vol. 26, pp.1294–1299, 2015.

[37] V. Sharma. "A Review on Characterization of Solid Dispersion," International Journal of Engineering Applied Sciences and Technology, vol. 04, no. 6, pp. 127–128, 2019.

[38] G. M. Pinto and R. Nazareth. "Green synthesis and characterization of zinc oxide nanoparticles", Journal of chemical and Pharmaceutical Research, vol. 8, no. 6, pp. 427-432, 2016.

[39] A. F. Abdulrahman. "The Influence of Various Reactants in the Growth Solution on the Morphological and Structural Properties of ZnO Nanorods", Passer Journal, Vol. 2 (2), pp. 69-75, 2020. doi: 10.24271/psr.14

[40] A. F. Abdulrahman, S. M. Ahmed, A. A. Barzinjy, S. M. Hamad, N. M. Ahmed, M. A. Almessiere. "Fabrication and Characterization of High-Quality UV Photodetectors Based ZnO Nanorods Using Traditional and Modified Chemical Bath Deposition Methods", Nanomaterials, vol. 11, no.3, pp. 677, 2021. https://doi.org/10.3390/nano11030677

[41] A. F. Abdulrahman, N. M. Abd-Alghafour."Synthesis and characterization of ZnO nanoflowers by using simple spray pyrolysis technique", Solid-State Electronics, vol. 189, pp.108225, 2022. https://doi.org/10.1016/j.sse.2021.108225.

[42] J. P. Kim, I. K. Lee, B. S. Yun, S. H. Chung, G. S. Shim, H. Koshino, I. D. Yoo. "Ellagic acid rhamnosides from the stem bark of Eucalyptus globulus", Phytochemistry, vol. 57, pp.587–591, 2001.

[43] S. A. Santos, S. F. Carmen, M. Rosário, M. Domingues, J. D. Armando, P. N. Carlos. "Characterization of phenolic components in polar extracts of Eucalyptus globulus Labill. Bark by high-performance liquid chromatography-mass spectrometry", J. Agric Food Chem., vol. 59, pp.9386–9393, 2011.

[44] L. Roza, Y. A. Rahman, A. A. Umar, M. M. Salleh. "Direct growth of oriented ZnO nanotubes by self-selective etching at lower temperature for photo-electrochemical (PEC) solar cell application", J. of Alloys and Comps., vol. 618, pp.153, 2015.

[45] R. Shabannia, H.A. Hassan. "Characteristics of photoconductive UV photodetector based on ZnO nanorods grown on polyethylene naphthalate substrate by a chemical bath deposition method", Electron. Mater. Lett., vol. 10, pp.837–843, 2014. https://doi.org/10.1007/s13391-014-3245-0.

[46] E. Pretsch, P. Bühlmann, C. Affolter, E. Pretsch, P. Bhuhlmann, C. Affolter. "Structure determination oforganic compounds", Springer, Berlin, p. 108, ISBN: 978-3-662-04201-4, 2000. https://doi.org/10.1007/978-3-662-04201-4.

[47] M. M. Khan. "Potentials of Costus woodsonii leaf extract in producing narrow band gap ZnO nanoparticles", Material Science Semicondutor Process., vol. 91, pp. 194200, 2019.

[48] N. Pantidos, L.E. Horsfall. "Biological synthesis of metallic nanoparticles by bacteria, fungi and plants", J. Nanomed. Nanotechnology, vol. 5, no.5, pp.1, 2014.

[49] J. Jiang, G. Oberdörster, A. Elder, R. Gelein, P. Mercer, P. Biswas. "Does nanoparticle activity depend upon size and crystal phase", Nanotoxicology, vol. 2, no. 1, pp. 33-42, 2008.

[50] D. Singh. "Synthesis, characterization and application of semiconducting oxide (Cu2O and ZnO) nanostructures", Bull. Material Science, vol. 31, no.3, pp. 319-325, 2008.

[51] A. Balcha, O. P. Yadav, T. Dey. "Photocatalytic degradation of methylene blue dye by zinc oxide nanoparticles obtained from precipitation and sol-gel methods", Environ. Science Pollut. Res. Int., vol. 23, no. 24, pp. 25485-25493, 2016.

List of Tables

Table 1: Lattice Parameters in addition to ZnO wurtzite-hexagonal Structure Characteristics of the ZnO Nanoparticle along with stronger Peaks Diffraction (100), (002), and (101) planes synthesized from Different Zinc Salts.

Sample	Peaks	FWHM	2θ	c (Å)	ζc%	a (Å)	ζa%	I (a.u.)	d (Å)
ZN	**100**	0.3936	31.9910	5.59	7.62	3.227	-0.46	632	2.795
ZA	**100**	0.3936	31.9219	5.603	7.84	3.23	-0.258	542	2.801
ZC	**100**	0.3936	31.8865	5.603	7.96	3.238	-0.150	1050	2.804
ZN	**002**	0.3936	34.6996	5.166	-0.55	2.982	-8.025	514	2.583
ZA	**002**	0.4920	34.6152	5.178	-0.32	2.989	-7.808	546	2.589
ZC	**002**	0.2952	34.629	5.176	-0.36	2.988	-7.844	249	2.588
ZN	**101**	0.3936	36.5253	4.916	-5.367	2.8384	-12.477	972	2.458
ZA	**101**	0.3936	36.4374	4.927	-5.147	2.8449	-12.274	934	2.464
ZC	**101**	0.1721	36.4562	4.925	-5.194	2.8436	-12.317	514	2.463

Table 2: The Volume, Dislocation Density, and Bond Length of the ZnO Nanoparticle alongside stronger Peaks Diffraction (100), (002), and (101) planes synthesized from Different Zinc Salts.

Sample	Peaks	V(Å^3)	δ ×10^{-5} (Å^{-2})	L (Å)
ZN	**100**	50.45	2.268	2.019
ZA	**100**	50.77	2.269	2.023
ZC	**100**	50.93	2.269	2.025
ZN	**002**	39.80	2.236	1.865
ZA	**002**	40.08	3.496	1.870
ZC	**022**	40.04	1.258	1.869
ZN	**101**	34.29	2.21	1.775
ZA	**101**	34.54	2.21	1.779
ZC	**101**	34.49	4.23	1.778

List of Figures

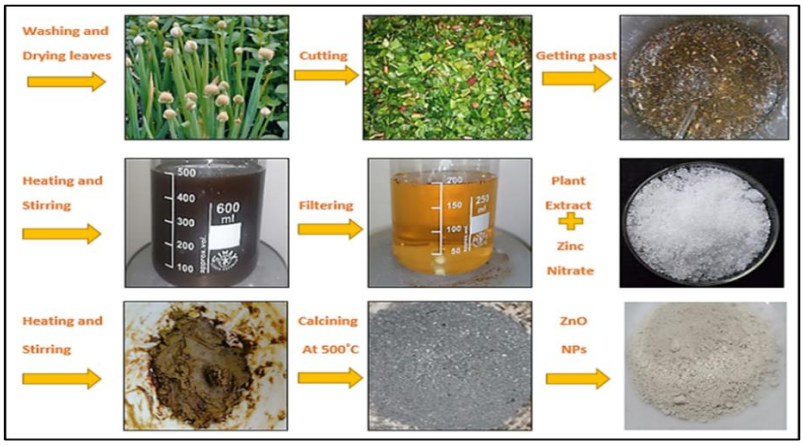

Figure 1: Schematic illustration of the ZnO NPs for Biosynthesis by means of the leaf extract of Allium Calocephalum Wendelbow in addition to Different Zinc Salts.

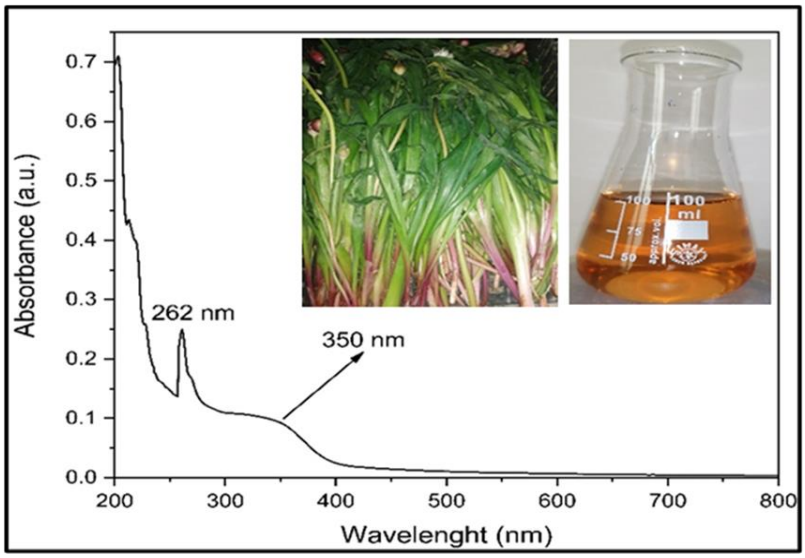

Figure 2: UV- Visible Spectrum of the Allium Calocephalum Wendelbow leaf extract.

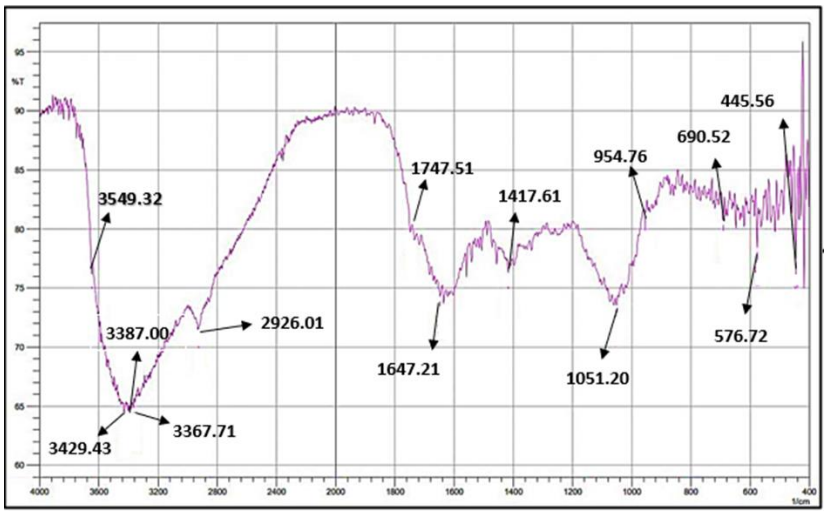

Figure 3: The FTIR Spectra of the Allium Calocephalum Wendelbow leaf extract.

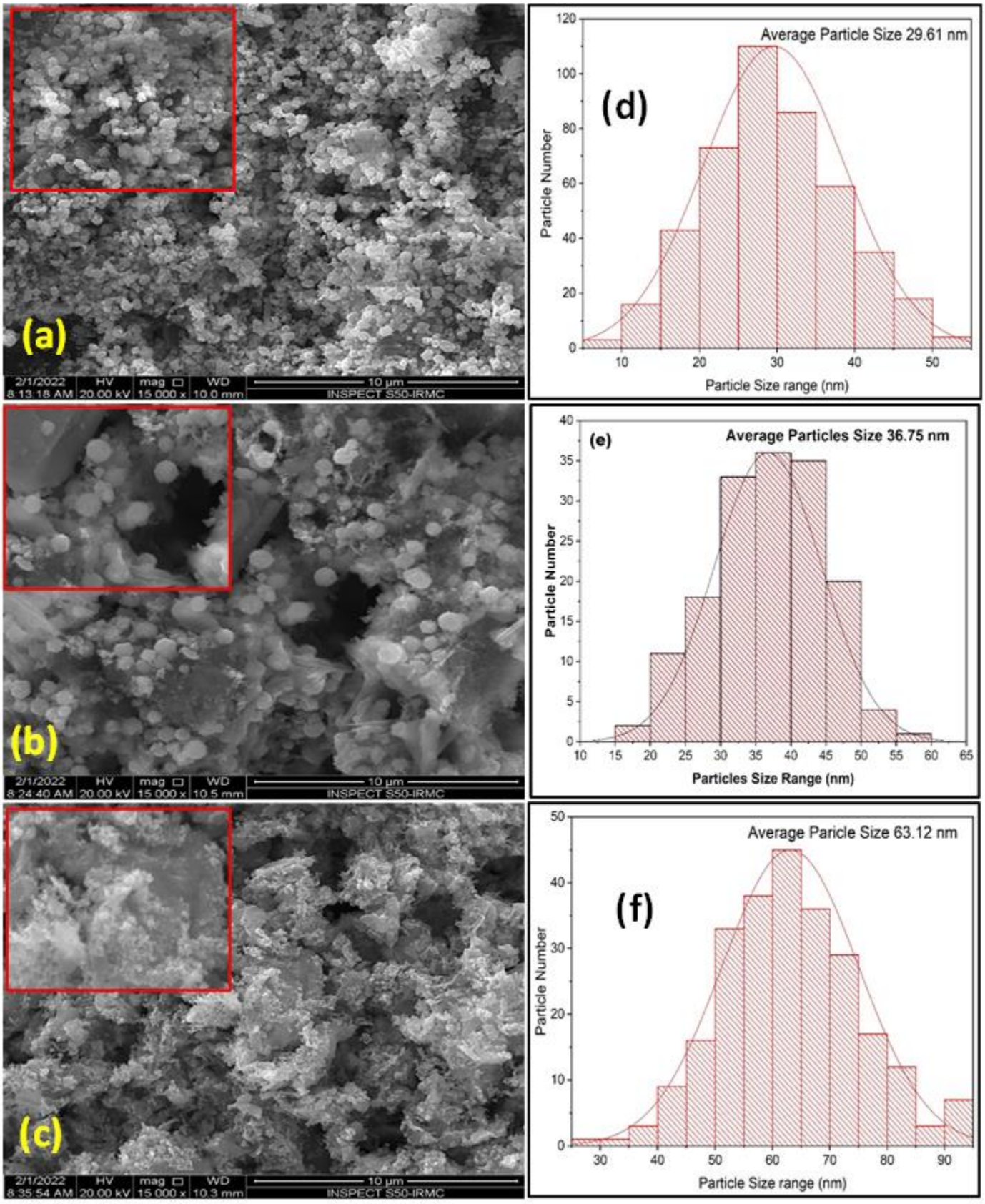

Figure 4: Top View FESEM Images of ZnO Nanoparticles synthesized by Green Method as of Dissimilar Zinc Salts: (a) Zinc Nitrate, (b) Zinc Acetate, and (c) Zinc Chloride. Frequency Histogram of ZnO NPs Distribution for Different Zinc Salts: (d) Zinc Nitrate, (e) Z.

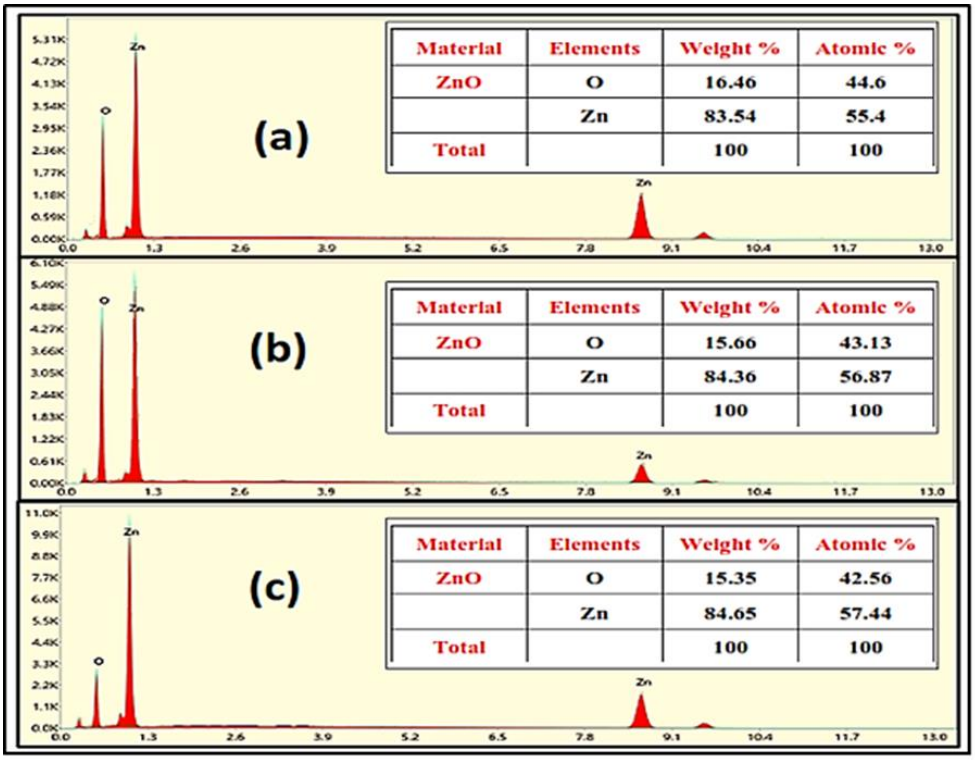

Figure 5: Typical EDX Analysis of ZnO Nanoparticles Equipped via Biosynthesis Way for Dissimilar Zinc Salts: (a) Zinc Nitrate, (b) Zinc Acetate, (c) Zinc Chloride.

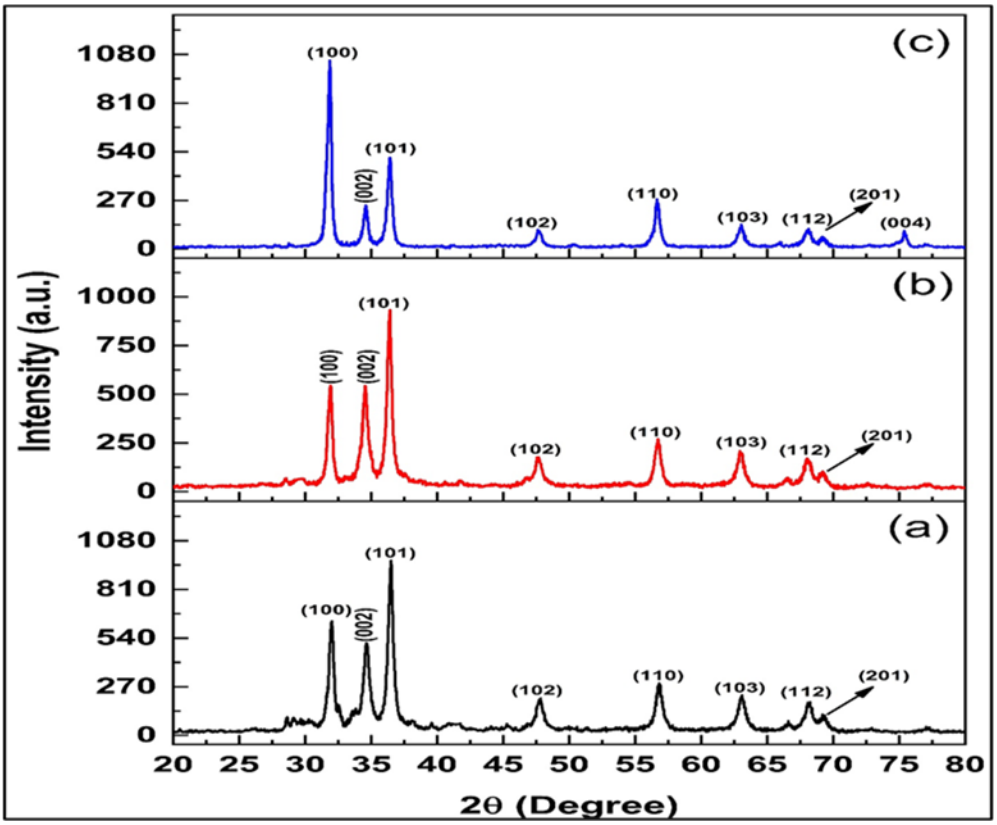

Figure 6: The pattern of XRD of the synthesized ZnO NPs employing ACW for different salts (a) Zinc Nitrate, (b) Zinc Acetate, also (c) Zinc Chloride.

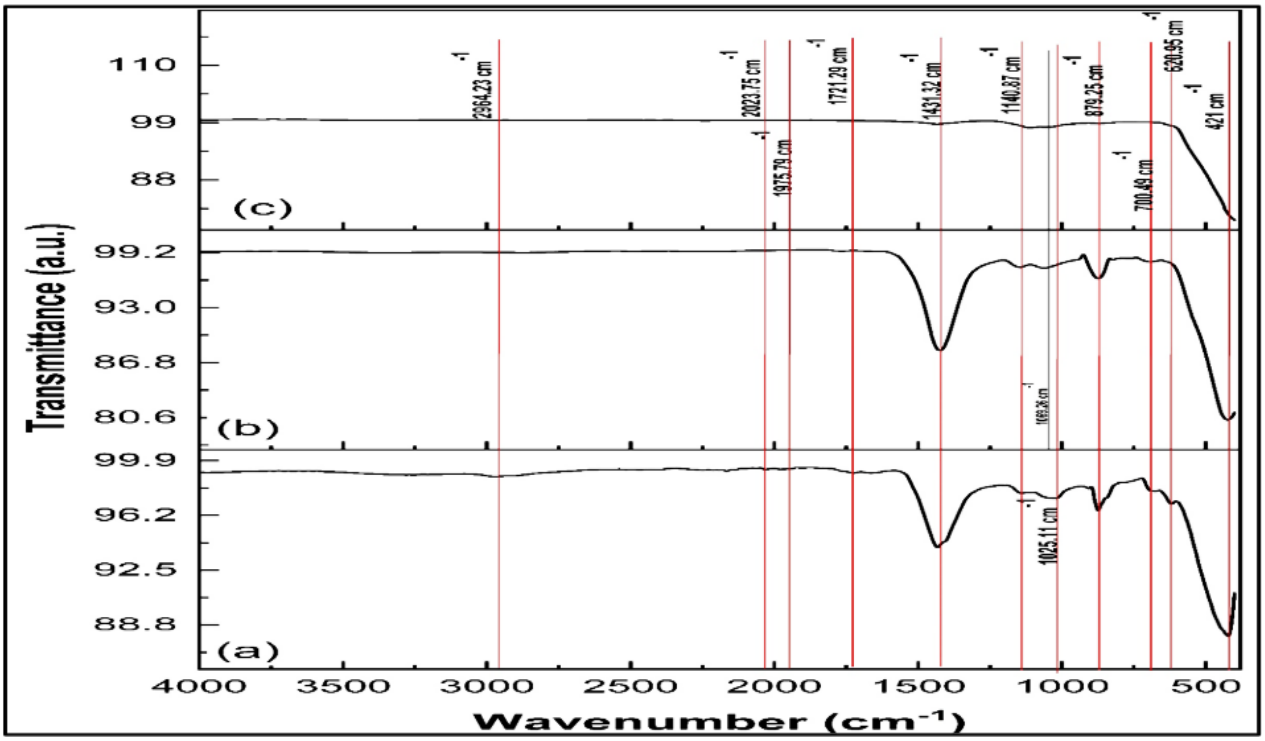

Figure 7: The FTIR Analysis Spectrums of the synthesized ZnO NPs by using ACW for different salts (a) Zinc Nitrate, (b) Zinc Acetate, also (c). Zinc Chloride.

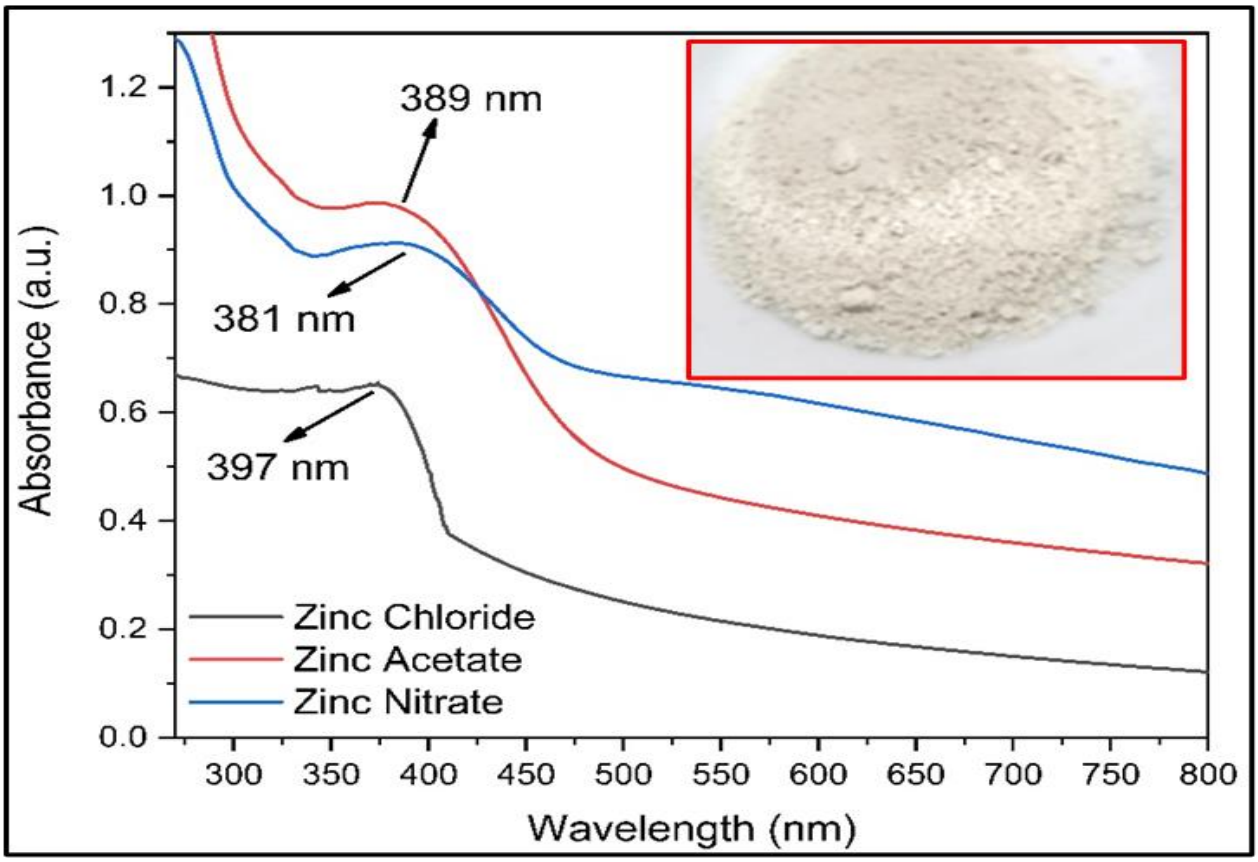

Figure 8: Optical Absorption Spectrums of the synthesized ZnO NPs by using ACW for different Zinc salts.

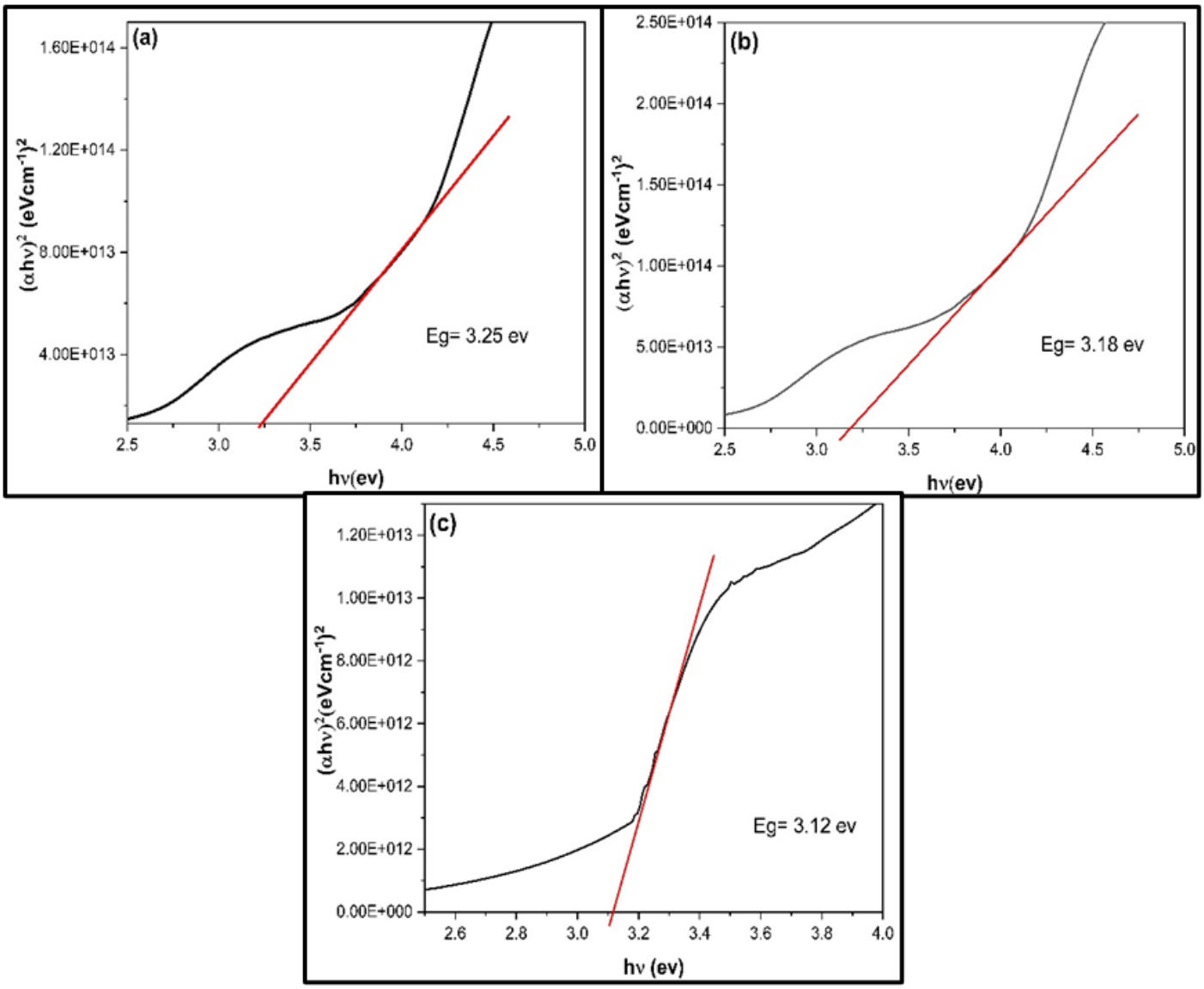

Figure 9: The Tauc-plot Versus Energy Band Gap of biosynthesized ZnO NPs by using Leaf extract of AWC as of Different Zinc Salts: (a) Zinc Nitrate, (b) Zinc Acetate, also (c) Zinc Chloride.